Vol. 46, No. 1 (2024) 29-38, DOI: 10.24874/ti.1483.05.23.08

Tribology in Industry

www.tribology.rs

RESEARCH

Fabrication and Sliding Wear Characterization of Eggshell Particulate Reinforced AA6061 Alloy Metal Matrix Composites

Chaman Lal[a], Sachin Tejyan[b,*], Vedant Singh[c]

[a]*Abhilashi University, Mandi, Himachal Pradesh 175028, India,*
[b]*G. B. Pant Institute of Engineering and Technology, Pauri, Uttarakhand 246194, India,*
[c]*Amrita Vishwa Vidyapeetham, Bengaluru, Karnataka 560035, India.*

Keywords:

Eggshell
Metal matrix composites
Stir casting
Mechanical properties
Sliding wear

* Corresponding author:

Sachin Tejyan
E-mail: tejyan86@gmail.com

Received: 19 May 2023
Revised: 29 June 2023
Accepted: 7 August 2023

A B S T R A C T

In this work, AA6061 aluminum alloy composites reinforced with industrial wastes, i.e., eggshell particles are fabricated. The stir casting technique was used to fabricate the Al6061 metal matrix composites. The AA6061 matrix contains 3, 5, and 7 wt.% eggshell particles as reinforcement. Mechanical characterization i.e., hardness, toughness, and tensile strength was examined of the eggshell particle-reinforced composites. According to the experimental findings, adding eggshell particles significantly increased the material's hardness, tensile strength, and toughness. Moreover, the sliding wear resistance improved by adding eggshell particles as reinforcement. ANNOVA results predict that sliding velocity and load are the dominant factors for the sliding wear of composites.

1. INTRODUCTION

Metal matrix composites are widely utilized in the aerospace, marine, and automotive industries because of their excellent stability at higher temperatures, high strength-to-weight ratio, low corrosion, and exceptional wear resistance [1]. For various industrial and aeronautical applications, metal matrix composites based on aluminum alloys and filled with diverse materials are currently being researched. Due to its high strength-to-weight ratio, an aluminum alloy from the 7xxx series called AA7075 is employed in the aerospace, defense, and military industries [2]. Although AA7075 has a high strength-to-weight ratio and outstanding fatigue properties, its usage is constrained by its average machinability, fair tribological properties, moderate wear resistance, and higher cost [3]. For aerospace and automotive applications, AA6061 is yet another popular aluminum alloy commonly used [4]. In these applications, aluminum alloys undergo different loading and surface delamination by wear. To overcome mechanical failures and wear losses, aluminum alloys were reinforced with different particles to make metal matrix composites for two decades [5,6].

Various scientists and researchers developed metal matrix composites by different fabrication techniques utilizing aluminium and its alloy as matrix material, and industrial wastes i.e. SiC [7,8,10,17], Al_2O_3 [7,9], TiB_2 [11], TiC [12,13], WC [14], graphite [15], ZrB_2 [16], B_4C [17], steel dust [18], and zircon [19] etc. as filler materials. Shyamlal et al. [7] developed an AA359/Al_2O_3 metal matrix composite using the electromagnetic stir casting technique and evaluated its tensile strength, hardness, and microstructure. The hardness and tensile strength of the composites improve with an increase in alumina weight percentage, as microstructures confirm the homogeneous distribution of alumina. A. Kumar et al. [20] have fabricated and characterized Al-4.5% Cu/10TiC composite by in situ method. The base metal has aluminium 4.5 wt.%, copper alloy, and 10 wt.% TiC is used as the reinforcement. Improvement in yield strength, ultimate tensile strength, and hardness was reported to be about 15, 24, and 35 % respectively. Tejyan et al. [21] developed AA6063-based metal matrix composites with the help of powdered industrial waste (SiC, 2, 4, and 6 wt.%) and natural waste (neem leaf ash, 2, 3, and 4 wt.%). According to experimental results, SiC and neem leaf ash powders improved tensile strength, impact strength, and hardness. According to C. Kapil et al. [22], 30% of marble must be recovered from mining to finishing in the production process. To examine the impact of marble dust reinforcement in metal matrix composites, the author discovered that aluminium alloy metal matrix composites can effectively use marble dust as reinforcement.

S.B. Hassan et al. [23] fabricated composites with varying reinforcement of eggshell in Al-Cu-Mg. They found that density, hardness, tensile strength, and impact strength increase with the addition of carbonized and un-carbonized eggshell powder. Moreover, carbonized eggshell powder gives better mechanical properties than un-carbonized eggshell powder reinforced composites. Other authors [24-26] also successfully utilized eggshell powder as reinforcement in different aluminium alloys and found an improvement in composites' mechanical and wear behavior. The composite material created by incorporating different filler materials into the AA6061 matrix has better mechanical characteristics than the original aluminium alloy in terms of strength, and stiffness [25]. Therefore, using particle-reinforced AA6061 composites in manufacturing lightweight structural parts for automobiles, such as engine components, chassis parts, and body panels may be advantageous [24,25].

Based on the various studies related to aluminium alloy metal matrix composites reinforced with various particles such as SiC, TiB_2, eggshell, rise husk, and marble dust, no study has been found related to the development and characterization of AA6061 aluminium alloy metal matrix composites reinforced with eggshell powder. This work aims to stir-cast AA6061 metal matrix composites reinforced with carbonized eggshell particles and describe the mechanical and sliding wear behaviour.

2. MAIN EXPERIMENTAL PROCEDURE

2.1 Materials and fabrication of composites

AA6061 aluminum alloy (Density: 2.70 g/cm^3, Yield strength: 145 MPa) supplied by Gayatri Industries, Roorkee, India is used as matrix material. Micro-image and chemical compositions of AA6061 aluminum alloy are presented in Figure 3(a), and Table 1 respectively. For the composites, shown in Figure 1, the naturally occurring bio-waste eggshell powder (density: 2.0 g/cm$_3$) is utilized as filler material. By weight, the eggshell's chemical makeup consists of 94% calcium carbonate, 1% magnesium carbonate, 4% organic content, and 1% calcium phosphate. The eggshell was cleaned and dried in a furnace at 40° C to remove the moisture. The dried eggshell was ball milled at 250 rpm to create an eggshell powder. The carbonaceous elements were removed by carbonization at 600°C for 4 hours. According to Figure 2, the EDS of the carbonized eggshell particles reveals that the particles consist of Si, Ca, Mg, C, and O. It also shows that the size of the carbonized eggshell powder is smaller than the un-carbonized eggshell powder. Additionally, these components confirm that the eggshell particles are composed of calcite ($CaCO_3$), a type of calcium carbonate.

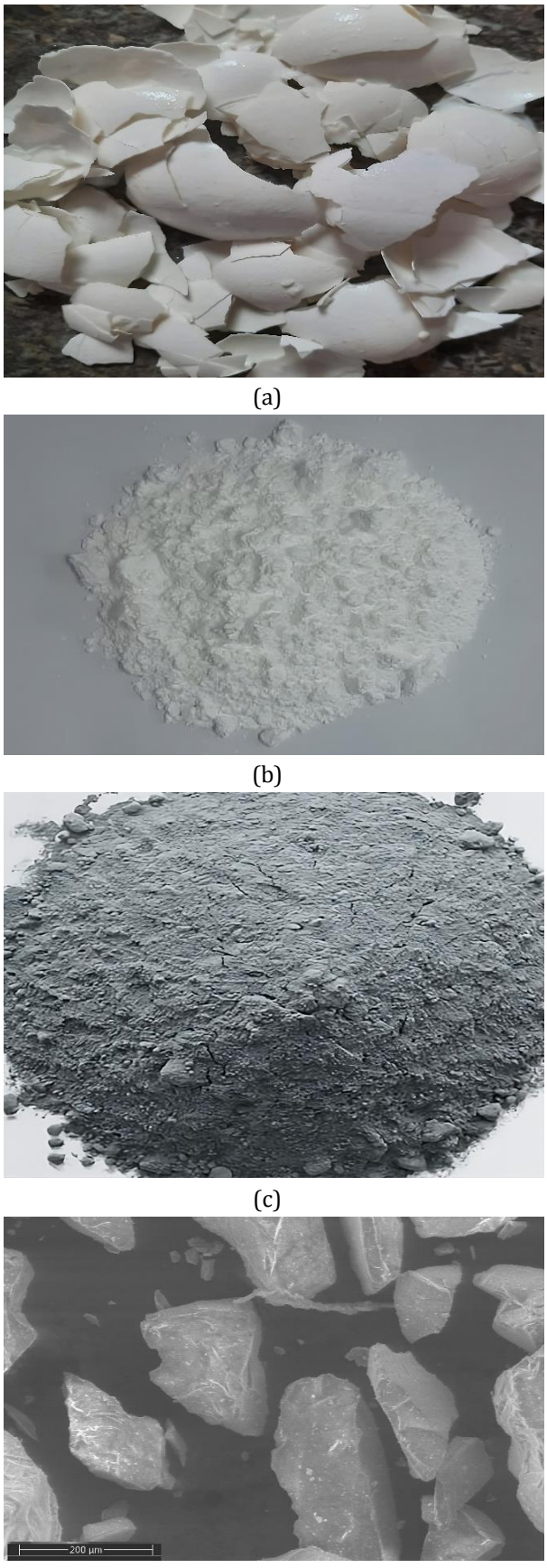

(a)

(b)

(c)

(d)

Fig. 1. (a) Eggshell, (b) Un-carbonized eggshell powder, (c) Carbonized eggshell powder, and (d) Micro image of un-carbonized eggshell powder.

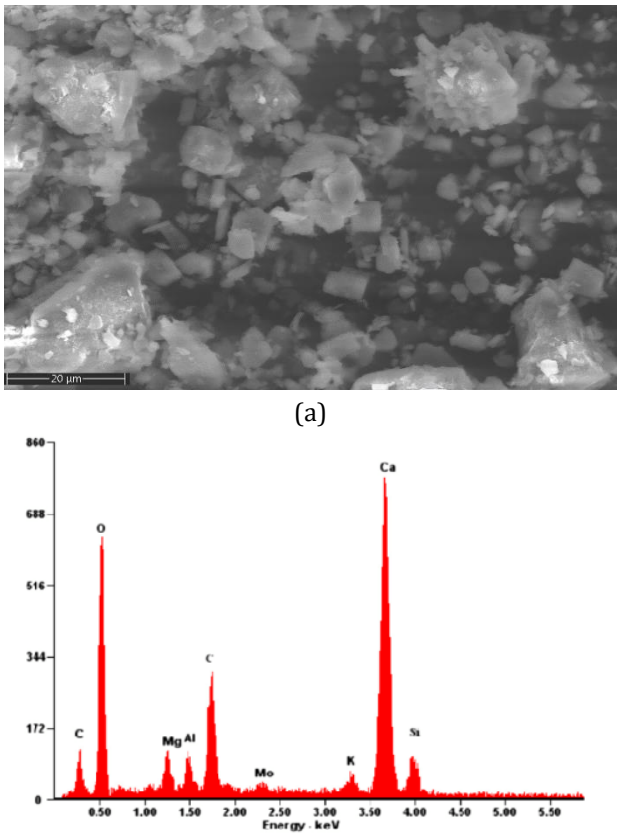

(a)

(b)

Fig. 2. Carbonized eggshell powder (a) SEM image and (b) EDS.

The mechanical stir casting technique is used to fabricate AA6061 metal matrix composites, Figure 4. Al6061 alloy is melted in the furnace and reinforcement material (Carbonized eggshell particles, Size: 200 µm) are added and mixed using an externally threaded stirrer (Material: stainless steel, Length: 100 mm, and Diameter: 25 mm). The mixture was mechanically stirred using a motor of around 250 rpm for 10 minutes before pouring into the mold. Fabricated composites (Plaque Size: 200×100 mm^2) with their composition and designation are present in Table 2. The microstructure of the fabricated composites is presented in Figure 3. The strong interfacial bond between the eggshell particles and the matrix material, and the eggshell particles' strong wettability with the molten aluminum alloy affect how the eggshell particles are distributed. The eggshell particles are evenly dispersed along the grain boundaries of the composites' microstructures [23]. The kinetics of reactions determine how the components of eggshell particles react with a molten aluminum alloy matrix. As a result of the carbonized eggshell particles' tiny size compared to un-carbonized eggshell particles, it should be noted that the

presence of carbonized eggshell particles causes the grain size in the cast composites to be significantly smaller [2].

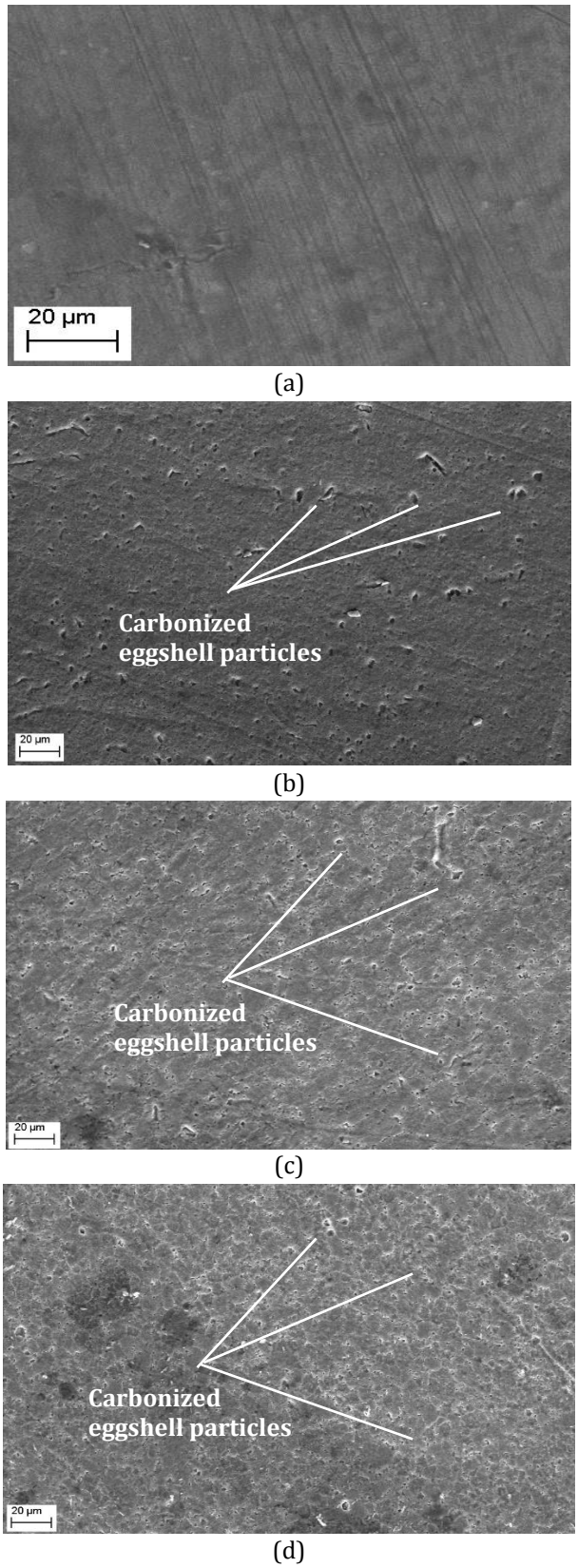

Fig. 3. Micro images of fabricated composites (a) EC1; (b) EC2; (c) EC3; and (d) EC4.

2.2 Material characterization

Hardness, impact, and tensile strength were determined on samples cut from the casted rectangular plaque (size: 200×100 mm^2). The impact strength of fabricated composite specimens was determined using the Charpy impact test on an impact tester (TINIUS OLSEN India Pvt. Ltd., Model No. IT406) following the ASTM-E23 standard. The tensile strength of produced composite samples was tested using an ASTM-E8-compliant Universal Testing Machine (Hounsfield Test Equipment Limited, England, Model H25K-S). The micro-hardness of the specimens was determined using an ASTM-E384 micro-hardness tester (Duramin-40 A2, Struers, LLC, United States) [22].

Table 1. Elemental composition of Al6061.

Element	Wt.%
Mg	1.00
Si	0.60
Fe	0.70
Mn	0.27
Cr	0.15
Zn	0.20
Ti	0.15
Others	0.08
Al	96.60

Table 2. Composition and designation of fabricated composites.

Designation	Composition
EC1	100 wt.% Al6061 + 0 wt.% Eggshell
EC2	97 wt.% Al6061 + 3 wt.% Eggshell
EC3	95 wt.% Al6061 + 5 wt.% Eggshell
EC4	93 wt.% Al6061 + 7 wt.% Eggshell

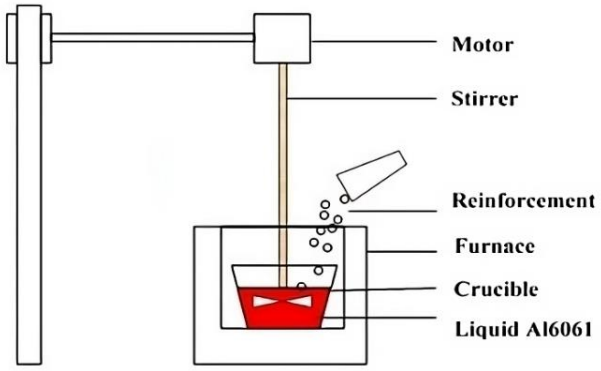

Fig. 4. Schematic diagram of stir casting of Al6061 and eggshell composites.

2.3 Pin-on-disc wear test

The wear rates under dry sliding conditions were simulated using a pin-on-disc tribometer (Model: TR20, Ducom, India) following the ASTM-G99 standard. As shown in Figure 5, the tribometer comprises an EN-31 hardened steel disc. The composite pin that is being loaded is forced against the counter-face steel disc that is continuously rotating. The steel disc is 60 HRC hard and has a surface roughness of 1.6 Ra. Composite specimen pins with dimensions of 8 mm in diameter and 30 mm in length were used for wear testing.

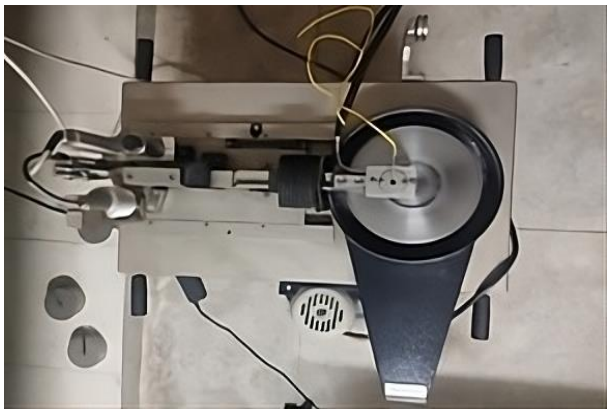

Fig. 5. Pin-on-disc apparatus for sliding wear test.

The weight of the composite pins was measured before and after the test using electronic weighing equipment with a 0.0001 g precision. The wear experiments were carried out with various loads (10, 20, 30, and 40 N) and sliding speeds (0.62, 1.25, 1.88, and 2.51 m/s) while keeping other parameters constant (Track radius: 40 mm, Temperature: ambient). The difference between the initial weight of the composite pin and the end weight served as the basis for calculating the mass loss (m) during wear tests. The wear loss is mathematically described by the following relation:

$$\Delta m = W_1 - W_2 \quad (1)$$

Where W_1 and W_2 are the weights of the composite pins before and after the wear test, respectively, and Δm is the total mass loss.

The wear rate is calculated by:

$$WR = \frac{\Delta m}{\rho \times L} \text{ mm}^3/\text{m} \quad (2)$$

Where WR stands for wear rate, Δm for mass loss in grams, ρ for composite density, and L for track length.

2.4 Process optimization and Taguchi method

Table 3. Levels of selected control factor.

Control factor	Level			
	I	II	III	IV
A: Eggshell (wt.%)	0	3	5	7
B: Normal Load (N)	05	10	15	20
C: Sliding Velocity (m/s)	150	300	450	600
D: Temperature (°C)	25	40	60	80

Table 4. L16 orthogonal array design for selected control parameters.

Ex. No.	A: Eggshell (wt.%)	B: Normal load (N)	C: Sliding velocity (m/s)	D: Temperature (°C)
1	0	5	150	25
2	0	10	300	40
3	0	15	450	60
4	0	20	600	80
5	3	5	300	60
6	3	10	150	80
7	3	15	600	25
8	3	20	450	40
9	5	5	450	80
10	5	10	600	60
11	5	15	150	40
12	5	20	300	25
13	7	5	600	40
14	7	10	450	25
15	7	15	300	80
16	7	20	150	60

On a pin-on-disc tribometer, a variety of control parameters are accessible for the evaluation of sliding wear rates. For this study, four control parameters with four levels each i.e. normal load, sliding speed, temperature, and marble dust wt.% were chosen. $4^4 = 256$ trials are required in a traditional complete factorial design to evaluate four control variables [27]. Taguchi's experimental design reduces this enormous number of experimental iterations. Here, the Minitab 18 program generated experimental runs using Taguchi analysis. Table 3 lists four chosen control factors, each with four levels. Using an L16 orthogonal array, the Taguchi experimental design allows for transforming 256 iterations into only 16 trials (Table 4). The signal-to-noise (S/N) ratio is then calculated using the experimental results regarding wear rate [15].

$$\frac{S}{N} = -10 \log \frac{1}{n}(\sum y_2) \quad (3)$$

Here, n is the number of observations, and y denotes observed wear loss.

2.5 Scanning electron microscopy (SEM)

Scanning Electron Microscope (Model No. FEI NOVA Nano-SEM 450, Lincoln, UK) is used to study the worn surfaces of the specimens. Before taking photomicrographs, a tiny layer of platinum is vacuum-evaporated and applied to the samples to improve their conductivity.

3. RESULT AND DISCUSSION

3.1 Density and voids in composites

The experimental and measured densities of the EC1, EC2, EC3, and EC4 composites are presented in Figure 6, which explores the reduction in both experimental and measured density due to the addition of low-density material (eggshell particles, density = 2.0 gm/cm^3) from 0 to 7 wt.% in EC1, EC2, EC3, and EC4 composites. Similar results were reported by previous works [23,24].

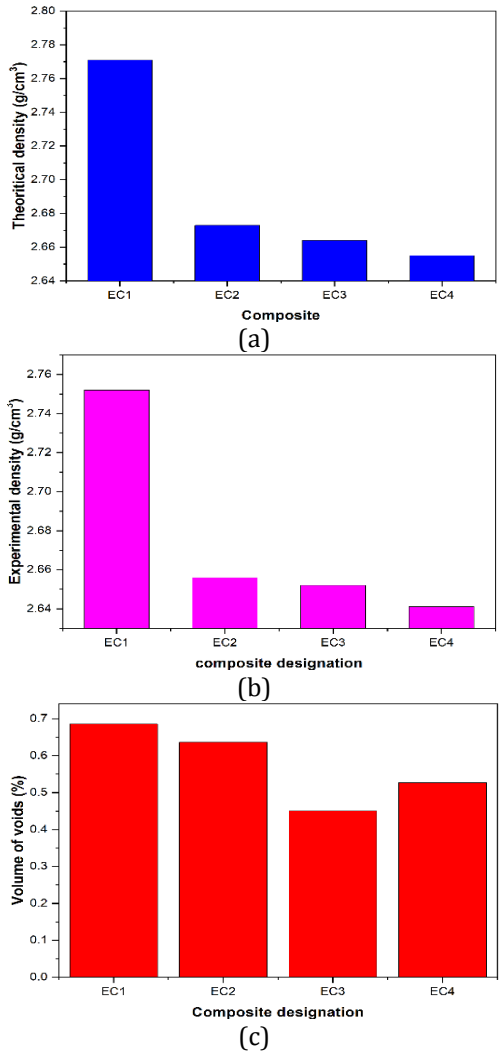

Fig. 6. (a) Theoretical density, (b) Experimental density, and (c) Volume of voids.

The void content in the composites is also reduced by adding the eggshell particles from 0 to 5 wt.%, it may be due to the proper mixing of eggshell particles and Al6061 metal alloy in liquid and solid forms [24,25]. Moreover, improved wettability, which encourages nucleation, and crystallization may be responsible for reducing the void percentage up to 5 wt.% eggshell composites [23]. Furthermore, wettability may decrease by 7 wt.% eggshell reinforcements and the void contents present in the composite increase.

3.2 Hardness and impact strength of fabricated composites

Figure 7 presents the Micro-hardness of the fabricated composites EC1, EC2, EC3, and EC4. It is seen that hardness improves with the addition of eggshell particles as reinforcement in the AA6061 alloy matrix, which may be due to the less void contents. Moreover, the highest hardness was reported for the EC4 composite having 7 wt.% of eggshells, i.e. 55 Hv, and the lowest hardness for the EC1 composite having 0 wt.% of eggshell, i.e. 43 Hv. The impact energy absorbed by the composites is also presented in Figure 7. Composite EC3 (5 wt.% eggshells) gives the highest impact energy value, at the same time, composite EC1 (0 wt.% eggshell) shows the most bass impact energy value [26]. The order of impact energy is 11 J < 13 J < 14.5 J < 16.5 J for the EC1, EC4, EC2, and EC3 composites, respectively. It might be due to the fewer void contents in the EC3 composite and with 5 wt.% eggshell reinforcements, there is a better distribution and dispersion of the particles within the metal matrix. This optimal distribution allows for effective load transfer between the matrix and the reinforcement particles, enhancing impact strength [23,24].

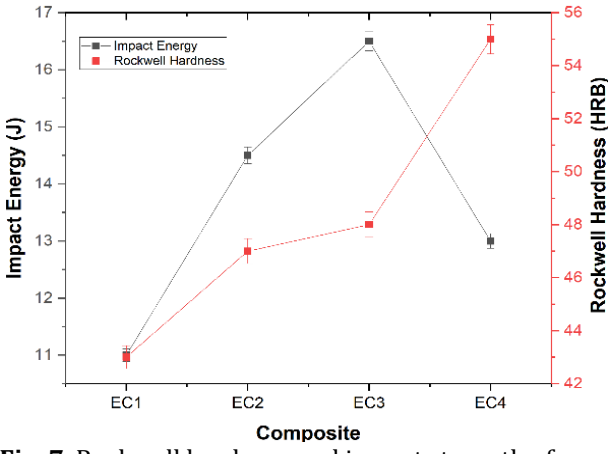

Fig. 7. Rockwell hardness and impact strength of composites.

3.3 Flexural strength and tensile strength of fabricated composites

Figure 8 presents the tensile strength of the fabricated composites (EC1, EC2, EC3, and EC4). The tensile strength shows slight improvement with the addition of eggshell particles in the AA6061 matrix phase. The highest tensile strength for the composite EC4 i.e., 257 MPa, whereas the lowest for the EC1 composite i.e. 245 MPa. The tensile strength improves in order of 245 MPa < 252 MPa < 255 MPa < 257 MPa for EC1, EC2, EC3, and EC4 composites. This improvement in the tensile strength may be due to the accumulation of eggshell particles and fewer voids in higher eggshell particle content composite [7-9].

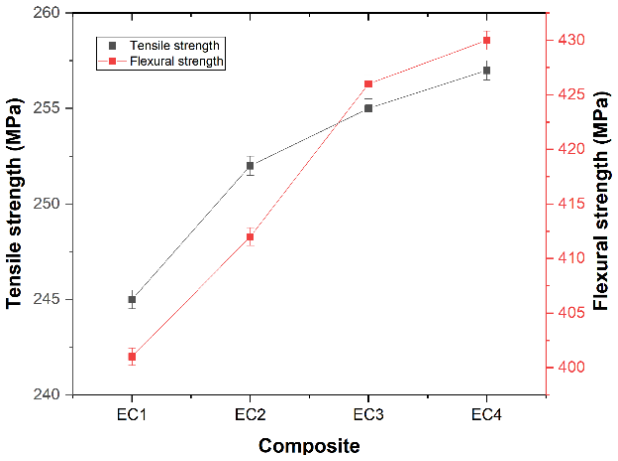

Fig. 8. Tensile and Flexural strength of composites.

The flexural strength of EC1, EC2, EC3, and EC4 composites is also presented in Figure 8, which shows a similar profile as tensile strength and improves with the addition of eggshell particles. Flexural strength improves by adding eggshell particles from 3 to 7 wt.% for the EC2, EC3, and EC4 composites. The flexural strength improves in order of 401 MPa < 412 MPa < 426 MPa < 430 MPa for the EC1, EC2, EC3, and EC4 composites respectively. It could result from a perfect balance between particle-particle interactions and matrix bonds. The composites' tensile and flexural strength is increased due to this balanced interaction's improved load transfer [25].

3.4 Effect of control parameters on sliding wear of composites

Table 5 presents the specific wear rate with the corresponding S-N Ratio for the L16 orthogonal array designed as per the selected control parameter i.e. A: Eggshell weight, B; Normal load, C: Sliding velocity, and D: Temperature. The average S-N ratio for the L16 orthogonal array is 59.592 dB, as in Table 5. After the analysis of the S-N Ratio Table 6 presents the ranking of selected control parameters, which clearly indicates A: Normal load is the most dominating factor. The ranking of control parameters in terms of dominance and significance is 1, 2, 3, and 4 for B: Normal load, A: Eggshell weight, D: Temperature, and C: Sliding velocity respectively.

Table 5. S-N ratio of the L16 orthogonal array.

Ex. No.	Specific Wear Rate (mm^3/m)	S-N Ratio (dB)
1	0.00064	63.876
2	0.00101	59.913
3	0.00154	56.249
4	0.00177	55.040
5	0.00081	61.830
6	0.00126	57.992
7	0.00135	57.393
8	0.00124	58.131
9	0.00075	62.498
10	0.00089	61.012
11	0.00105	59.576
12	0.00132	57.588
13	0.00072	62.853
14	0.00096	60.354
15	0.00101	59.913
16	0.00109	59.251
	Mean S-N Ratio	**59.592**

Table 6. Ranking of control parameters.

Level	Eggshell (wt.%)	Normal Load (N)	Sliding velocity (m/s)	Temp. (°C)
1	58.77	62.76	60.17	59.8
2	58.84	59.82	59.81	60.12
3	60.17	58.28	59.31	59.59
4	60.59	57.5	59.07	58.86
Delta	1.82	5.26	1.1	1.26
Rank	2	1	4	3

Table 7 shows the percentage contribution of individual control parameters on the wear rate of composites. It's indicated by Table 7, that parameter B: Normal load has the highest contribution (71.34%) for the wear of composites. Moreover, other parameters i.e. A: Eggshell weight, C: Sliding

velocity, and D: Temperature having 11.37, 3.24, and 3.77% contribution respectively for the wear of composites, similar results were reported by S. Basavarajappa et al. [15]. Moreover, Figure 9 presents the combination of control factors by which fabricated composites possess the highest wear resistance. The factor combination A4, B1, C1, and D2 i.e. (7 wt.% marble dust, 10 N normal load, 0.53 m/s sliding velocity, and 30°C temperature) gives the least amount of sliding wear of composites.

Table 7. ANNOVA table and percentage contribution of selected control parameters.

Source	DF	Adj SS	Adj MS	F-Value	P-Value	Contribution (%)
Eggshell (wt.%)	3	10.32	3.44	1.11	0.468	**11.37**
Normal Load (N)	3	64.77	21.59	6.94	0.073	**71.34**
Sliding velocity (m/s)	3	2.93	0.97	0.31	0.816	**03.24**
Temperature (°C)	3	3.42	1.14	0.37	0.784	**03.77**
Error	3	9.33	3.11	--	--	**10.28**
Total	15	90.80	--	--	--	**100.00**

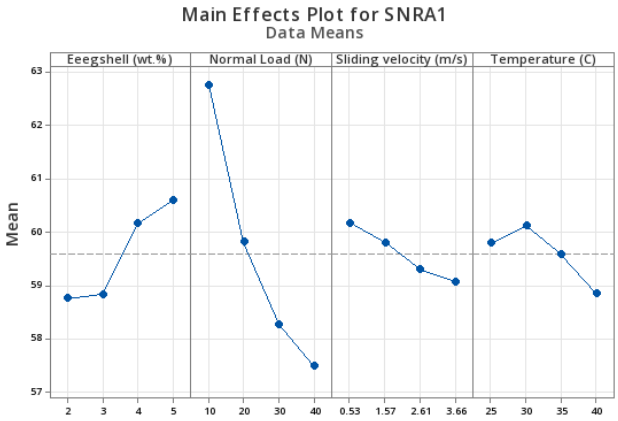

Fig. 9. Main effect plot for S-N ratios of control parameters.

3.5 Morphology of wear surface of composites

The morphology of composites' wear surfaces is presented in Figure 10 for the EC1, EC2, EC3, and EC4 composites respectively. Figure 8(a) presents the wear surface micrograph of the EC1 (Pure AA6061) composite, which shows wear tracks clearly. Figure 8(b) presents the wear surface of the EC2 (3 wt.% eggshells) composite, which clearly shows the eggshell particles present in the AA6061 metal matrix. The pin-on-disc disc's wear tracks are also present on the surface of EC2 composites. A micrograph of the wear surface of EC3 (5 wt.% eggshell) is present in Figure 8(c) and indicates ploughing and segregation of filler material are the main phenomena for the wear of composite [16-17]. Moreover, Figure 8(d) presents the surface morphology of the EC4 (7 wt.%) composite, which shows surface delamination is the phenomenon for the wear of the composite [24,25].

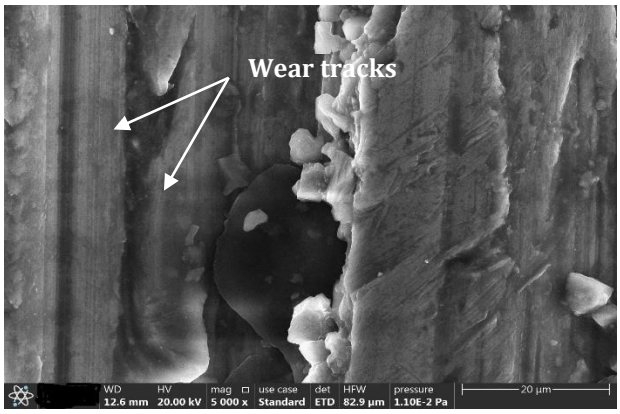

(a)

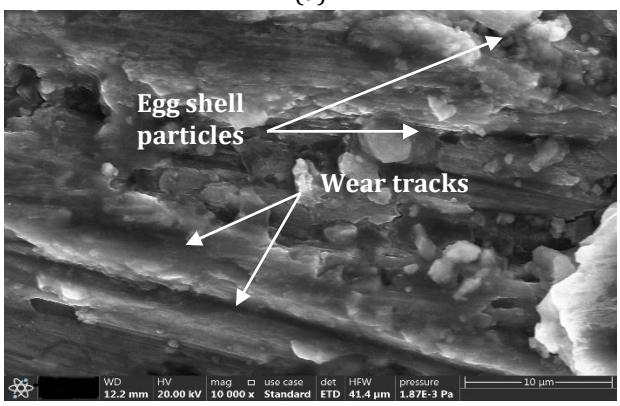

(b)

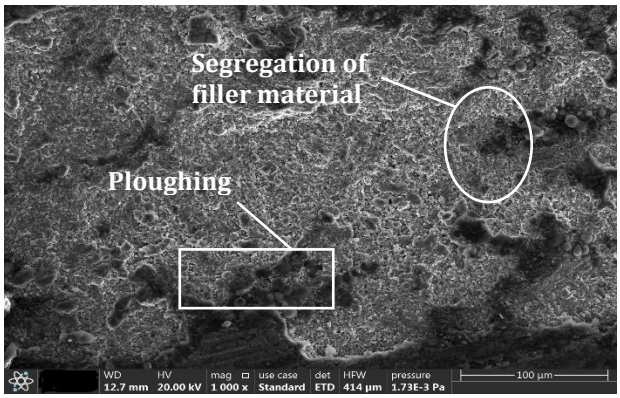

(c)

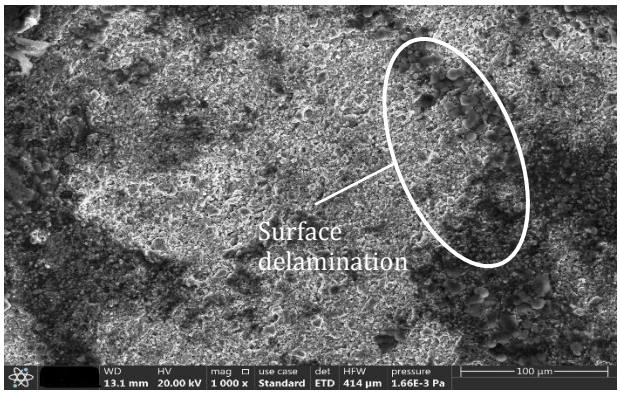

(d)

Fig. 10. Micrograph of wear surfaces (a) EC1; (b) EC2; (c) EC3; and (d) EC4 composite.

4. CONCLUSION

The mechanical stir casting technique produced AA6061 metal matrix composites reinforced with different weight percentages of eggshell particles. The mechanical properties of the developed composites, such as hardness, tensile strength, flexural strength, and impact energy, have been examined, and the following findings have been drawn. The EC4 composite shows the highest hardness, tensile strength, and flexural strength compared to the EC1, EC2, and EC3 composites. Moreover, the impact strength of the EC3 composite is highest compared to other composites. Overall EC4 composite presents great mechanical properties compared to the EC1, EC2, and EC3 composites. Regarding the sliding wear of composites, the normal load has the biggest influence on the wear rate of composites. Whereas wear track, ploughing, and surface delamination are the major cause of the wear of fabricated composites.

REFERENCES

[1] H. Khan *et al.*, "Investigating the microstructural and mechanical properties of novel Ternary reinforced AA7075 Hybrid Metal Matrix Composite," *Materials*, vol. 15, no. 15, p. 5303, Aug. 2022, doi: 10.3390/ma15155303.

[2] M. Aamir, K. Giasin, M. Tolouei-Rad, and A. Vafadar, "A review: drilling performance and hole quality of aluminium alloys for aerospace applications," *Journal of Materials Research and Technology*, vol. 9, no. 6, pp. 12484–12500, Nov. 2020, doi: 10.1016/j.jmrt.2020.09.003.

[3] R. Bertolini, E. Simonetto, L. Pezzato, A. Fabrizi, A. Ghiotti, and S. Bruschi, "Mechanical and corrosion resistance properties of AA7075-T6 sub-zero formed sheets," *The International Journal of Advanced Manufacturing Technology*, vol. 115, no. 9–10, pp. 2801–2824, May 2021, doi: 10.1007/s00170-021-07333-7.

[4] A. Baradeswaran, S. C. Vettivel, A. Perumal, N. Selvakumar, and R. F. Issac, "Experimental investigation on mechanical behaviour, modelling and optimization of wear parameters of B4C and graphite reinforced aluminium hybrid composites," *Materials in Engineering*, vol. 63, pp. 620–632, Nov. 2014, doi: 10.1016/j.matdes.2014.06.054.

[5] M. Ọlayinka Durowoju *et al.*, "Improving mechanical and thermal properties of graphite–aluminium composite using Si, SiC and eggshell particles," *Journal of Composite Materials*, vol. 54, no. 17, pp. 2365–2376, Dec. 2019, doi: 10.1177/0021998319892058.

[6] N. H. Ononiwu, E. T. Akinlabi, and C. G. Ozoegwu, "Sustainability in Production and Selection of Reinforcement particles in Aluminium Alloy Metal Matrix Composites: A Review," *Journal of Physics*, vol. 1378, no. 4, p. 042015, Dec. 2019, doi: 10.1088/1742-6596/1378/4/042015.

[7] S. Lal, S. Kumar, and Z. A. Khan, "Microstructure evaluation, thermal and mechanical characterization of hybrid metal matrix composite," *Science and Engineering of Composite Materials*, vol. 25, no. 6, pp. 1187–1196, Aug. 2018, doi: 10.1515/secm-2017-0210.

[8] S. Hao and J. Xie, "Tensile properties and strengthening mechanisms of SiCp-reinforced aluminum matrix composites as a function of relative particle size ratio," *Journal of Materials Research*, vol. 28, no. 15, pp. 2047–2055, Jul. 2013, doi: 10.1557/jmr.2013.202.

[9] S. A. Sajjadi, H. R. Ezatpour, and H. Beygi, "Microstructure and mechanical properties of Al–Al_2O_3 micro and nano composites fabricated by stir casting," *Materials Science and Engineering: A*, vol. 528, no. 29–30, pp. 8765–8771, Nov. 2011, doi: 10.1016/j.msea.2011.08.052.

[10] T. P. D. Rajan, R. M. Pillai, and B. C. Pai, "Characterization of centrifugal cast functionally graded aluminum-silicon carbide metal matrix composites," *Materials Characterization*, vol. 61, no. 10, pp. 923–928, Oct. 2010, doi: 10.1016/j.matchar.2010.06.002.

[11] M. Emamy, M. Mahta, and J. Rasizadeh, "Formation of TiB_2 particles during dissolution of $TiAl_3$ in Al–TiB_2 metal matrix composite using an in situ technique," *Composites Science and Technology*, vol. 66, no. 7–8, pp. 1063–1066, Jun. 2006, doi: 10.1016/j.compscitech.2005.04.016.

[12] P. N. Siddappa, B. P. Shivakumar, K. B. Yogesha, M. Mruthunjaya, and D. P. Girish, "The effect of TiC particulate reinforcement on dry sliding wear behaviour of Al based composites," *Materials Today: Proceedings*, vol. 22, pp. 2291–2299, Jan. 2020, doi: 10.1016/j.matpr.2020.03.350.

[13] J.D.R. Selvam, I. Dinaharan, R.S. Rai, P.M. Mashinini, "Dry Sliding Wear Behaviour of In-Situ Fabricated TiC Particulate Reinforced AA6061 Aluminium Alloy," *Tribology-Materials, Surfaces & Interfaces*, vol. 13, pp. 1-11, Nov. 2019, doi: 10.1080/17515831.2018.1550971.

[14] T. B. Rao and G. R. Ponugoti, "Characterization, prediction, and optimization of dry sliding wear behaviour of AL6061/WC composites," *Transactions of the Indian Institute of Metals*, vol. 74, no. 1, pp. 159–178, Nov. 2020, doi: 10.1007/s12666-020-02107-3.

[15] S. Basavarajappa, G. Chandramohan, and J. P. Davim, "Application of Taguchi techniques to study dry sliding wear behaviour of metal matrix composites," *Materials in Engineering*, vol. 28, no. 4, pp. 1393–1398, Jan. 2007, doi: 10.1016/j.matdes.2006.01.006.

[16] R. Kumar, R. Keshavamurthy, C. S. Perugu, M. A. Alipour, and C. Siddaraju, "Influence of hot rolling on friction and wear behaviour of Al6061-ZrB_2 in-situ metal matrix composites," *Journal of Manufacturing Processes*, vol. 69, pp. 473–490, Sep. 2021, doi: 10.1016/j.jmapro.2021.07.058.

[17] M. Khare, R.K. Gupta, B. Bhardwaj, "Dry Sliding Wear Behaviour of Al 7075/Al_2O_3/B_4C Composites Using Mathematical Modelling and Statistical Analysis," *Materials Research Express*, vol. 6, pp. 126512, Nov. 2019, doi: 10.1088/2053-1591/ab546a.

[18] S. O. Adeosun, E. I. Akpan, O. I. Sekunowo, W. A. Ayoola, and S. A. Balogun, "Mechanical characteristics of 6063 Aluminum-Steel Dust Composite," *ISRN Mechanical Engineering (Print)*, vol. 2012, pp. 1–9, Aug. 2012, doi: 10.5402/2012/461853.

[19] T. S. P. Kumar, S. Shalini, G. Priyadharshini, and R. Raghu, "Parametric optimization of dry sliding wear behavior of A356 Alloy-Zircon Composites," *Tribology in Industry*, vol. 44, no. 4, pp. 719–730, Dec. 2022, doi: 10.24874/ti.1348.08.22.11.

[20] A. Kumar, M. M. Mahapatra, and P. K. Jha, "Fabrication and Characterizations of Mechanical Properties of Al-4.5%Cu/10TiC Composite by In-situ Method," *Journal of Minerals and Materials Characterization and Engineering*, vol. 11, no. 11, pp. 1075–1080, Jan. 2012, doi: 10.4236/jmmce.2012.1111113.

[21] S. Tejyan, Ch. Kapil. Ror, and N. K. K. Kumar, "Mechanical properties of SiC and neem leaf powder reinforced Al-6063 hybrid metal matrix composites," *Materials Today: Proceedings*, vol. 60, pp. 884–888, Jan. 2022, doi: 10.1016/j.matpr.2021.09.521.

[22] Ch. Kapil. Ror, S. Tejyan, and N. K. K. Kumar, "Effect of marble dust reinforcement in composites for different applications: A review," *Materials Today: Proceedings*, vol. 60, pp. 1120–1124, Jan. 2022, doi: 10.1016/j.matpr.2022.02.246.

[23] S.B. Hassan, V.S. Aigbodion, "Effects of Eggshell on the Microstructures and Properties of Al–Cu–Mg/Eggshell Particulate Composites," *Journal of King Saud University – Engineering Sciences*, vol. 27, pp. 49–56, Jan. 2015, doi: 10.1016/j.jksues.2013.03.001.

[24] S. P. Dwivedi, S. Sharma, and R. K. Mishra, "Effects of waste eggshells and SiC addition in the synthesis of aluminum hybrid green metal matrix composite," *Green Processing and Synthesis*, vol. 6, no. 1, pp. 113–123, Dec. 2016, doi: 10.1515/gps-2016-0119.

[25] M. T. Hayajneh, M. Almomani, and M. M. Al-Shrida, "Effects of Waste Eggshells addition on Microstructures, Mechanical and Tribological Properties of Green Metal Matrix Composite," *Science and Engineering of Composite Materials*, vol. 26, no. 1, pp. 423–434, Jan. 2019, doi: 10.1515/secm-2019-0027.

[26] N. H. Ononiwu, C. G. Ozoegwu, N. Madushele, and E. T. Akinlabi, "Carbonization Temperature and Its Effect on the Mechanical Properties, Wear and Corrosion Resistance of Aluminum Reinforced with Eggshell," *Journal of Composites Science*, vol. 5, no. 10, p. 262, Oct. 2021, doi: 10.3390/jcs5100262.

[27] S. Tejyan, "Effect of Erosive Parameters on Solid Particle Erosion of Cotton Fiber–Based Nonwoven Mat/Wooden Dust Reinforced Hybrid Polymer Composites," *Journal of Industrial Textiles*, vol. 51, pp. 2514-2532, Dec. 2021, doi: 10.1177/1528083721106424.